journal

J. Am. Ceram. Soc., 77 [7] 1897–900 (1994)

Effects of Fiber Volume Fraction on Mechanical Properties of SiC-Fiber/Si_3N_4-Matrix Composites

Hockin H. K. Xu,† Claudia P. Ostertag,* and Linda M. Braun*

National Institute of Standards and Technology, Gaithersburg, Maryland 20899

Isabel K. Lloyd*

Department of Materials and Nuclear Engineering, University of Maryland, College Park, Maryland 20742

The effects of fiber volume fraction on composite mechanical properties were examined in SiC-fiber-reinforced Si_3N_4 composites fabricated in our laboratories. Fiber volume fraction was found to have significant effects on important composite properties including failure mode, ultimate strength, matrix-cracking stress, fiber–matrix interfacial shear stress, and work-of-fracture. The composite mechanical properties were improved with increasing fiber volume fraction. However, when the fiber volume fraction was sufficiently large, the composite ultimate strength was degraded. This was related to fiber strength loss as a result of fiber damage from contact with surrounding fibers and abrasive matrix particles during hot pressing.

I. Introduction

It is now well-established that ceramic materials can be substantially toughened by reinforcing them with strong, continuous fibers. With weak fiber–matrix interfaces, the toughening effect comes from the closure stress across the crack planes exerted by the bridging fibers. This closure stress depends on fiber volume fraction, f. Fiber volume fraction affects the toughening and other mechanical properties of the composites. Theories of continuous-fiber ceramic composites (CFCCs) predict that the composite ultimate strength, σ_u, is linearly proportional to fiber volume fraction f.[1–5] Experimental results on the effects of fiber volume fraction, on the other hand, have been contradictory. Shetty *et al.*[6] studied hot-pressed Si_3N_4-matrix composites reinforced with SCS-2 SiC fibers. They found that the composite strength is virtually independent of fiber volume fraction f from $f \approx 5\%$ to $f = 45\%$. In contrast, Dawson *et al.*[7] studied hot-pressed SiC-fiber-reinforced glass-matrix composites and found that composite strength increased linearly with f from $f \approx 20\%$ to $f \approx 60\%$. Recently Hegeler *et al.*[8] found in their hot-pressed SiC-fiber/glass-matrix composites that the composite strength increased with f, reaching a maximum at $f \approx 50\%$, and then decreased rapidly with further increase of f. An understanding of the influence of fiber volume fraction is therefore needed, both to better understand CFCC behavior and to guide composite processing for tailored properties.

This paper presents results on the effects of fiber volume fraction on mechanical properties of SiC-fiber/Si_3N_4-matrix composites, including failure mode, ultimate strength, matrix-cracking stress, interfacial shear stress, and work-of-fracture. The measured ultimate strength as a function of fiber volume fraction is compared with the theoretical prediction. The cause of the degradation of composite ultimate strength at high fiber volume fraction is related to fiber damage during sample fabrication.

II. Experimental Procedure

Unidirectional SiC-fiber (SCS-6, Textron Special Materials, MA)[‡]-reinforced Si_3N_4 composites were fabricated by hot pressing at 1650°C for 30 min in 0.1 MPa of N_2, as described elsewhere.[9] Composites with three different fiber loadings were fabricated. Mechanical testing was carried out in four-point flexure. The dimensions of the specimens were approximately 2.5 mm × 2.7 mm × 25 mm. The inner and outer spans of the test fixture were 10 and 20 mm, respectively. Testing was performed using a universal Instron machine. A constant displacement rate of 0.5 mm/min was used. Load–displacement curves were recorded. Four specimens of each type were tested and the results averaged. Crack–fiber interactions, specimen fracture surface, and fiber fracture surface were examined by scanning electron microscopy (SEM).

III. Mechanical Properties

The composite mechanical properties investigated in this study include composite failure mode, ultimate strength, matrix-cracking stress, fiber–matrix interfacial frictional shear stress, work-of-fracture, and fiber bundle strength. Composite failure mode (whether failure is catastrophic or noncatastrophic) can be seen from the measured load–displacement curves of composites. The matrix-cracking stress, σ_c, can be obtained from the first load-drop point on the load–displacement curve.[9] The first load-drop was found to correspond to a traversed crack extending over the entire tensile surface of the specimen.[9] The work-of-fracture can be taken to be the area under the load–displacement curve divided by the specimen cross-sectional area.

The fiber–matrix interfacial shear stress, τ, can be obtained using the Aveston–Cooper–Kelly (ACK) theory.[14] This theory applies when the composite specimens show parallel matrix cracks normal to the fibers before specimen failure. The average spacing between these parallel cracks, d, can be used to estimate the fiber–matrix interfacial shear stress, τ:

$$\tau = [(1 - f)/f](\sigma_c R/2d) \quad (1)$$

where R is the fiber radius. This equation has been widely used to calculate τ.

R. Raj—contributing editor

Manuscript No. 194129. Received October 15, 1993; approved February 28, 1994.
Based in part on the Ph.D. dissertation of H. H. K. Xu.
Supported by the Department of Energy, Office of Industrial Technology, under Contract No. DE A C05-840 R21400.
*Member, American Ceramic Society.
†Guest scientist from the Department of Materials and Nuclear Engineering, University of Maryland, College Park, Maryland 20742.

‡Certain trade names and products of companies are identified in this paper to adequately specify the materials and equipment used in this research. In no case does such identification imply that the products are necessarily the best for the purpose or that they are recommended by NIST.

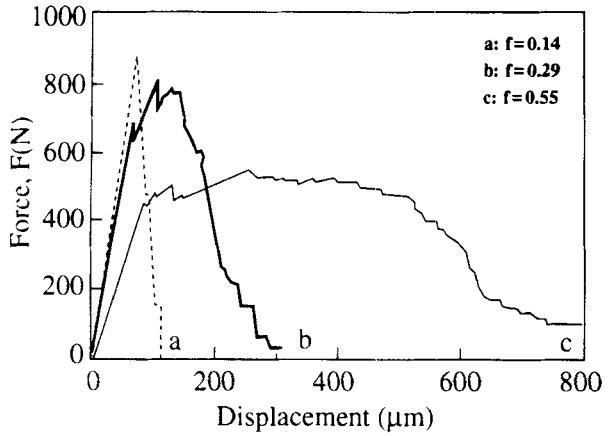

Fig. 1. Load–displacement curves of comp14 (curve a), comp29 (curve b), and comp55 (curve c).

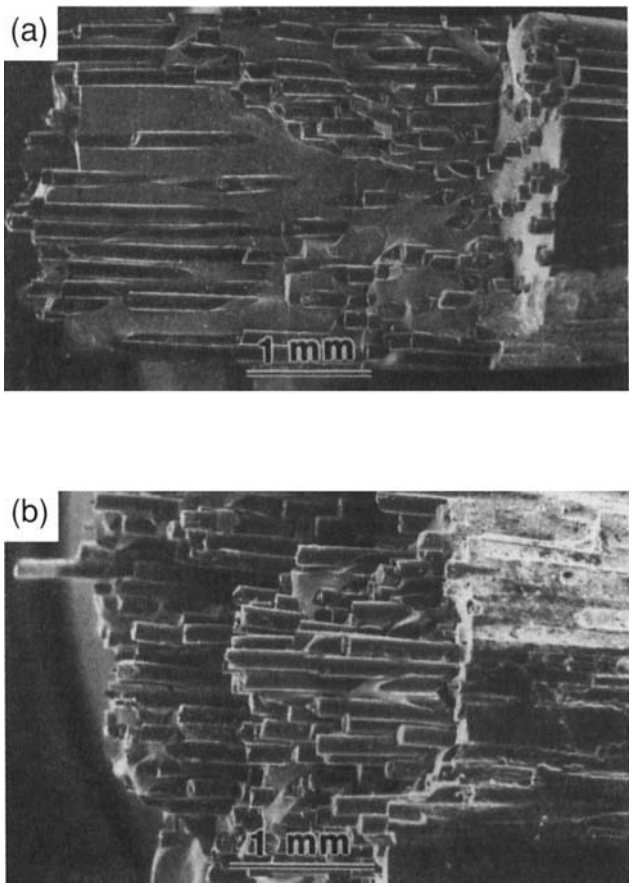

Fig. 2. Fracture surface of specimens of (a) comp29, and (b) comp55.

The composite ultimate strength, σ_u, can be obtained using the peak load on the load–displacement curve. In the case of *noncatastrophic* failure, this measured ultimate strength σ_u is equal to the fiber bundle strength, S_{fb}.[9] The fiber bundle strength is the load-carrying capability of the fibers in the composite, defined as[1–5,9,15]

$$S_{fb} = \alpha f S \tag{2}$$

where α is a dimensionless constant depending on fiber strength distribution, and S is the average strength of the fibers. In the case of catastrophic failure, the fibers cannot survive the onset of matrix cracking and fail in the wake of the crack tip. In this case $\sigma_u = \sigma_c > S_{fb} = \alpha f S$. Combining the two cases, the composite ultimate strength can be written as[9,15]

$$\sigma_u = \begin{cases} S_{fb} \text{ (with noncatastrophic failure, when } S_{fb} = \alpha f S > \sigma_c) & (3a) \\ \sigma_c \text{ (with catastrophic failure, when } S_{fb} = \alpha f S < \sigma_c) & (3b) \end{cases}$$

and the composite failure mode can be predicted by comparing the values of S_{fb} and σ_c.

IV. Results and Discussion

The average fiber volume fractions of the three composites fabricated were 14%, 29%, and 55%, and the three composites are therefore denoted "comp14," "comp29," and "comp55," respectively. Fiber distribution was not uniform, as described elsewhere.[9] Typical load–displacement curves for the three composites are shown in Fig. 1. As can be seen from these curves, comp14 exhibited brittle fracture, while comp29 and comp55 showed noncatastrophic failure. Values of σ_c and σ_u obtained from the load–displacement curves are listed in Table I, together with the work-of-fracture values.

Both comp29 and comp55 specimens showed extensive fiber bridging and pullout. However, there is a distinct difference in the fracture surface of the comp29 and comp55 specimens, as can be seen in Figs. 2(a) and (b). The fracture surface of comp29 showed "two-region" behavior, where the first region of the fracture surface was flat and normal to the reinforcing fibers, and the second region delaminated along the fibers. This phenomenon has been observed by other investigators.[12,13] In contrast, crack delamination was not observed in the comp55 specimens. The fracture surface of the comp55 specimens was basically normal to the fibers through the entire specimen thickness. The fiber pullout length was much longer in comp55 specimens than in comp29 specimens. This suggests that the fiber–matrix interfacial shear stress is lower in the comp55 than in comp29.

Comp14 specimens failed from a single crack, while both comp29 and comp55 specimens showed parallel matrix cracks normal to the fibers before failure. The fiber–matrix interfacial shear stress, τ, for comp29 and comp55 were obtained from Eq. (1), using the average measured spacing d values. For comp14, it was not possible to measure d since specimens failed from a single crack. Thus an upper bound for τ of comp14 was estimated taking 1/2 of the inner span to be d. These τ values are listed in Table I.

Experimental values of S_{fb} can be obtained from the load–displacement curves for comp29 and comp55 since failure is noncatastrophic and $S_{fb} = \sigma_u$. For comp14, S_{fb} cannot be obtained from the load–displacement curve in Fig. 1 since failure is catastrophic, so it was measured using an indentation-strength technique,[9] where σ_c is lowered by controlled-flaws so that failure became noncatastrophic. The measured values of S_{fb} are listed in Table I.

Table I. Mechanical Properties of SiC-Fiber/Si_3N_4-Matrix Composites at Various Volume Fractions

f*	Failure mechanism	σ_c (MPa)†	σ_u (MPa)‡	WOF (kJ/m²)§	τ (MPa)¶	S_{fb} (MPa)**
0.14 ± 0.01	Catastrophic	682 ± 45	682 ± 45	3.5 ± 0.1	<29	313 ± 7
0.29 ± 0.03	Noncatastrophic	531 ± 49	607 ± 70	12.1 ± 3.6	15	607 ± 70
0.55 ± 0.03	Noncatastrophic	361 ± 54	410 ± 89	19.0 ± 7.5	4	410 ± 89

*Fiber volume fraction. †Matrix cracking stress. ‡Composite ultimate strength. §Work-of-fracture. ¶Interfacial shear stress. **Fiber bundle strength.

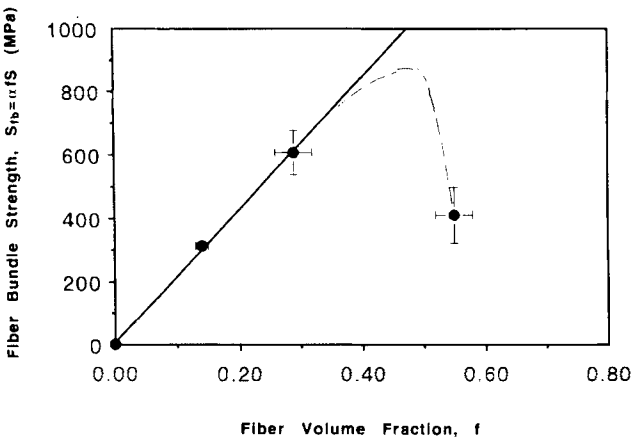

Fig. 3. Fiber bundle strength $S_{fb} = \alpha fS$ vs fiber volume fraction. Solid straight line shows linear relation of Eq. (2). Dotted curve illustrates a possible trend of experimental data.

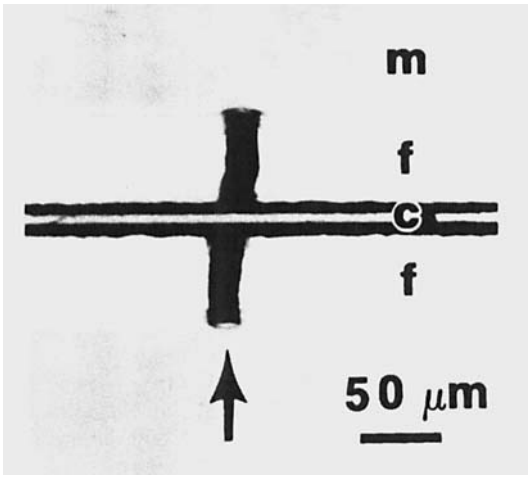

Fig. 5. Crack in a reinforcing SiC fiber: m = matrix, f = fiber, c = the carbon core of the fiber; the arrow points to a crack in the fiber.

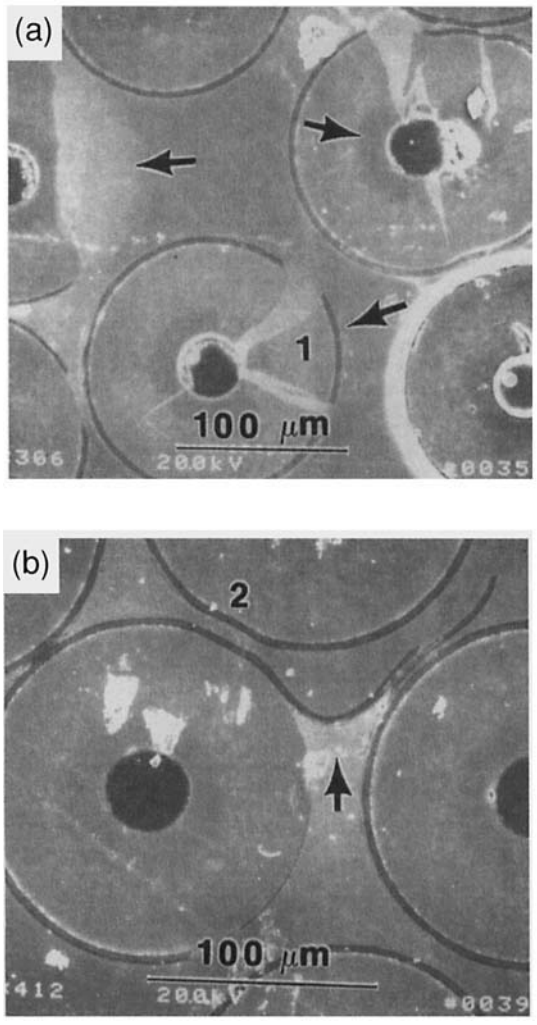

Fig. 4. SEM pictures showing fiber damage. Arrows show broken fibers in (a), and broken fiber coating in (b). "1" is a broken fiber, and "2" is a fiber that is squeezed out of shape, although there is a layer of matrix material surrounding it.

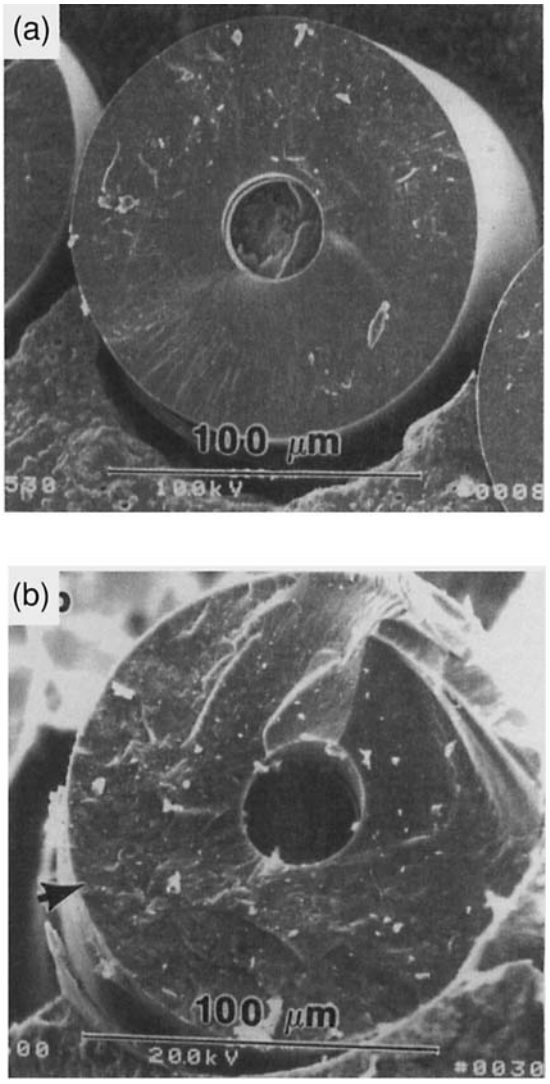

Fig. 6. Fracture surface of fibers in the composite: (a) fracture initiated near the interface of SiC and the carbon core of the fiber (comp29); (b) fracture initiated from outer surface damage (comp55). The arrow in (b) points to the possible damage area.

Figure 3 is a plot of the measured S_{fb} values versus fiber volume fraction f. The solid straight line shows the linear relation of Eq. (2). The dotted curve is for illustration, showing a possible trend. From $f = 14\%$ to 29%, S_{fb} increased linearly with increasing f, agreeing with the prediction of Eq. (2). However, when f was increased to 55%, S_{fb} ($= \sigma_u$) became much smaller than what the extrapolated linear relation predicts.

In examining the reasons for the degradation of S_{fb} and σ_u, microscopy revealed that some of the reinforcing fibers were damaged in the comp55 specimens. Figure 4(a) shows examples of broken fibers, and Fig. 4(b) shows fiber coating damage. Note that fiber "1" in Fig. 4(a) is broken, and fiber "2" in Fig. 4(b) is squeezed out of shape, although there is a layer of matrix material surrounding these fibers. There are two other manifestations of fiber damage. One is that there are cracks in the fibers on the specimen polished surface. An example of this is shown in Fig. 5. This was observed in both comp29 and comp55 specimens, but it is significantly more common in comp55 specimens. Another manifestation of fiber damage is the different fractographic appearance of the fiber fracture surface. Almost all the fibers in comp29 specimens examined failed from intrinsic flaws near the interface of SiC and the carbon-core of the fiber, as can be seen in Fig. 6(a). Most of the fibers examined in comp55 still fractured in this same manner, but there was a significant number of fibers that failed from outer surface damage; an example is shown in Fig. 6(b).

These observations suggest two reasons for the degradation of S_{fb} and σ_u at high fiber volume fractions in hot-pressed composites. First, fiber contact damage lowers fiber strength S in Eq. (2). Second, the damage widens the range of the fiber strength distribution and lowers the Weibull modulus, thereby lowering the value of α in Eq. (2). Therefore, both S and α in Eq. (2) are dependent on fiber volume fraction f and are sensitive to processing. Hence the relation between S_{fb} (hence σ_u) and f should not be simply taken as linear, and previous experimental observations[6–8] of the f dependence of σ_u should be analyzed and understood by taking into account the f dependence of S and α. The present investigation also suggests that the relation of both S and α with f is dependent on the hardness of the matrix particles, on the uniformity of fiber distribution in the composite, and on the hot-pressing pressure and temperature. Processing parameters (fiber volume fraction, temperature, pressure, etc.) need to be chosen to minimize fiber damage.

In summary, important mechanical properties were investigated as a function of fiber volume fraction in SiC-fiber/Si_3N_4-matrix composites. Composite mechanical properties were improved with the increase of fiber volume fraction. But when the fiber volume fraction was too large, the composite fiber bundle strength and hence ultimate strength degraded. This degradation was related to fiber damage from contacts with neighboring fibers and abrasive matrix particles during hot pressing.

Acknowledgments: We are very grateful to Dr. Brian R. Lawn and Dr. Sheldon M. Wiederhorn for discussion and help. We also thank Dr. Jerry Chuang, Dr. David Cranmer, Dr. Stephen Freiman, George Quinn, and Ralph F. Krause, Jr., at NIST for helpful discussions.

References

[1]A. G. Evans and D. B. Marshall, "The Mechanical Behavior of Ceramic Matrix Composites," *Acta Metall.*, **37** [10] 2567–83 (1989).

[2]M. D. Thouless, O. Sbaizero, L. S. Sigl, and A. G. Evans, "Effects of Interface Mechanical Properties on Pullout in a SiC-Fiber-Reinforced Lithium Aluminum Silicate Glass-Ceramic," *J. Am. Ceram. Soc.*, **72** [4] 525–32 (1989).

[3]P. S. Steif and H. R. Schwietert, "Ultimate Strength of Ceramic-Matrix Composites," *Ceram. Eng. Sci. Proc.*, **11** [9–10] 1567–76 (1990).

[4]W. A. Curtin, "Theory of Mechanical Properties of Ceramic-Matrix Composites," *J. Am. Ceram. Soc.*, **74** [11] 2837–45 (1991).

[5]K. M. Knowles and X. F. Yang, "Mathematical Modeling of the Strength and Toughness of Unidirectional Fiber-Reinforced Ceramics," *Ceram. Eng. Sci. Proc.*, **12** [7–8] 1375–88 (1991).

[6]D. K. Shetty, M. R. Pascucci, B. C. Mutsuddy, and R. R. Wills, "SiC Monofilament-Reinforced Si_3N_4 Matrix Composites," *Ceram. Eng. Sci. Proc.*, **6** [7–12] 632–45 (1985).

[7]D. M. Dawson, R. F. Preston, and A. Purser, "Fabrication and Materials Evaluation of High Performance Aligned Ceramic Fiber-Reinforced, Glass-Matrix Composite," *Ceram. Eng. Sci. Proc.*, **8** [7–8] 815–21 (1987).

[8]H. Hegeler and R. Bruckner, "Fiber-Reinforced Glasses: Influence of Thermal Expansion of the Glass Matrix on Strength and Fracture Toughness of the Composites," *J. Mater. Sci.*, **25**, 4836–46 (1990).

[9]H. H. K. Xu, C. P. Ostertag, L. M. Braun, and I. K. Lloyd, "Short-Crack Mechanical Properties and Failure Mechanisms of Si_3N_4-Matrix/SiC-Fiber Composites," *J. Am. Ceram. Soc.*, **77** [7] 1889–96 (1994).

[10]D. B. Marshall, B. N. Cox, and A. G. Evans, "The Mechanics of Matrix Cracking in Brittle-Matrix Fiber Composites," *Acta Metall.*, **33** [11] 2013–21 (1985).

[11]H. C. Cao, E. Bischoff, O. Sbaizero, M. Rühle, A. G. Evans, D. B. Marshall, and J. J. Brennan, "Effects of Interfaces on the Properties of Fiber-Reinforced Ceramics," *J. Am. Ceram. Soc.*, **73** [6] 1691–99 (1990).

[12]T. Mah, M. G. Mendiratta, A. P. Katz, R. Ruh, and K. S. Mazdiyasni, "High-Temperature Mechanical Behavior of Fiber-Reinforced Glass-Ceramic-Matrix Composites," *J. Am. Ceram. Soc.*, **68** [9] C-248–C-251 (1985).

[13]K. M. Prewo, "Tension and Flexural Strength of Silicon Carbide Fiber-Reinforced Glass Ceramics," *J. Mater. Sci.*, **21**, 3590–600 (1986).

[14](a) J. Aveston, G. A. Cooper, and A. Kelly, "The Properties of Fiber Composites"; p. 15 in Conference Proceedings, National Physical Laboratory. IPC Science and Technology Press, 1971. (b) J. Aveston and A. Kelly, "Theory of Multiple Fracture of Fibrous Composites," *J. Mater. Sci.*, **8**, 352–62 (1973).

[15]H. H. K. Xu, L. M. Braun, C. P. Ostertag, R. F. Krause, Jr., and I. K. Lloyd, "Failure Modes of SiC-Fiber/Si_3N_4-Matrix Composites at Elevated Temperatures," *J. Am. Ceram. Soc.*, in press. □